Adv. Appl. Prob. **48,** 1045–1060 (2016)
*doi:*10.1017/apr.2016.64

FIRST-PASSAGE TIMES OF TWO-DIMENSIONAL BROWNIAN MOTION

STEVEN KOU,* *National University of Singapore*
HAOWEN ZHONG,** *Columbia University*

Abstract

First-passage times (FPTs) of two-dimensional Brownian motion have many applications in quantitative finance. However, despite various attempts since the 1960s, there are few analytical solutions available. By solving a nonhomogeneous modified Helmholtz equation in an infinite wedge, we find analytical solutions for the Laplace transforms of FPTs; these Laplace transforms can be inverted numerically. The FPT problems lead to a class of bivariate exponential distributions which are absolute continuous but do not have the memoryless property. We also prove that the density of the absolute difference of FPTs tends to ∞ if and only if the correlation between the two Brownian motions is positive.

Keywords: First-passage times; two-dimensional Brownian motion; default correlation

2010 Mathematics Subject Classification: Primary 60J65
Secondary 91B28

1. Introduction

Consider a two-dimensional Brownian motion

$$X_i(t) = x_i + \mu_i t + \sigma_i W_i(t), \qquad x_i > 0,\ i = 1, 2,$$

where $W_i(t)$ are standard one-dimensional Brownian motions and $\operatorname{cov}(W_1(t), W_2(t)) = \rho t$, $-1 < \rho < 1$. Let $\tau_i = \inf_{t\geq 0}\{t\colon X_i(t) = 0\}$, $i = 1, 2$. We are interested in computing the following quantities:

(i) the joint distribution of first-passage times

$$\mathbb{P}^{(x_1,x_2)}(\tau_1 \leq t_1,\ \tau_2 \leq t_2); \tag{1}$$

(ii) the distribution

$$\mathbb{P}^{(x_1,x_2)}(|\tau_1 - \tau_2| \leq t); \tag{2}$$

(iii) the distribution

$$\mathbb{P}^{(x_1,x_2)}(\tau^* \leq t), \quad \text{where } \tau^* = \min(\tau_1, \tau_2); \tag{3}$$

(iv) the joint moment

$$\mathbb{E}^{(0,0)}[(-J_1(\varepsilon_p))(-J_2(\varepsilon_p))]; \tag{4}$$

(v) the joint moment

$$\mathbb{E}^{(0,0)}[(-J_1(\varepsilon_{p_1}))(-J_2(\varepsilon_{p_2}))]. \tag{5}$$

Received 28 May 2015; revision received 19 November 2015.

* Postal address: Risk Management Institute and Department of Mathematics, National University of Singapore, 21 Heng Mui Keng Terrace, I^3 Building 04-03, Singapore 119613. Email address: matsteve@nus.edu.sg

** Postal address: Department of Industrial Engineering and Operations Research, Columbia University, 500 West 120th Street, New York, NY 10027, USA.

Here, $J_i(t) := \min_{0\le s\le t} X_i(s)$, $i = 1, 2$, ε_p denotes an exponential random variable with rate p, and ε_{p_1} and ε_{p_2} are independent. Both exponential random variables are independent of the Brownian motions. Throughout the paper, $\mathbb{P}^{(x_1,x_2)}$ and $\mathbb{E}^{(x_1,x_2)}$ denote the conditional probability and the conditional expectation when the Brownian motion starts from (x_1, x_2), respectively.

There are numerous applications for both (1) and (3) in finance. In structural models for credit risk, defaults are modeled as first-passage times of (geometric) Brownian motions or other more general jump-diffusion processes; see, for example, [17]. Structural models have been used to study default correlations and interactions among different companies; see [13] and [28] for models where investors have complete information, and [10] for an incomplete-information model. In particular, in [6] the authors characterized the correlation structure of multiple firms given incomplete information. As pointed out in [6], such investigation may involve significant computational costs; the numerical methods proposed allowed the authors of [6] to mitigate this computational problem. From (3), τ^* was used in [14] in pricing double lookback options. For applications of the structured model in credit risk and default correlations, we refer the reader to [6], [10], [13], [15], and [28]. For applications of pricing double lookback, see [14].

Partly motivated by the applications above, existing literature provide some solutions to (1)–(5) using different approaches; see Table 1. Note that, except for [14] and [24], in all the other references it is essentially assumed that $\mu_1 = \mu_2 = 0$. The difficulty partly lies in the fact that with nonzero drifts, the two-dimensional Brownian motion ceases to be a conformal martingale (see [20]).

In this paper we obtain the Laplace transform (or joint Laplace transform) of (1)–(3) by solving a nonhomogeneous modified Helmholtz equation in an infinite wedge. To a large extent, whether a partial differential equation (PDE) is solvable analytically depends on the boundary conditions. For the above modified Helmholtz equations, if the boundary conditions are on a disk then the analytical solution is well known. However, in the problem at hand, the boundary conditions are on an infinite wedge with an angle, rendering the PDE problem difficult to solve. Nevertheless, we give two solutions to the PDE problem, one based on the finite Fourier transform and the other on the Kontorovich–Lebedev transform (by extending the method used in [23] to the case of arbitrary drifts). The finite Fourier transform leads to a more efficient numerical algorithm to compute the distribution functions; see Section 3.

Apart from the contributions listed earlier, there are other new results in this paper. First, we compute $\mathbb{P}^{(x_1,x_2)}(\tau_1 \le t_1,\ \tau_2 \le t_2)$ by numerical Laplace transform inversion, based on which we extend the study of default correlation in [28] to the case of arbitrary drifts (see Section 3). Secondly, we prove that the density of $|\tau_1 - \tau_2|$ with $\tau_1, \tau_2 < \infty$ tends to ∞ if and only if $\rho > 0$ (see Theorem 3). Finally, we point out a link between the first-passage times and a class of bivariate exponential distribution that is absolutely continuous but does not have the lack of memory property; see Section 5.

The rest of the paper is organized as follows. A general PDE problem is solved in Section 2, where we also verify the existence and uniqueness of the solution. As special cases, the joint Laplace transform $\mathbb{E}^{(x_1,x_2)}[\mathrm{e}^{-p_1\tau_1-p_2\tau_2}]$, the joint Laplace transform $\mathbb{E}^{(x_1,x_2)}[\mathrm{e}^{-q\tau^*-s|\tau_1-\tau_2|}]$, and the Laplace transform $\mathbb{E}^{(x_1,x_2)}[\mathrm{e}^{-p\tau^*}]$ are given in Section 2.5. We present a numerical algorithm to compute $\mathbb{P}^{(x_1,x_2)}(\tau_1 \le t_1,\ \tau_2 \le t_2)$ as well as an application to study default correlation in Section 3. The Laplace transform of $|\tau_1 - \tau_2|$ is given in Section 4, where we also discuss the property of the density of $|\tau_1 - \tau_2|$ near 0. Section 5 provides a link between the first-passage times and a class of bivariate exponential distributions. For all proofs of lemmas and theorems, we refer the reader to [29].

TABLE 1: In this table we summarize existing results on the first-passage time problem of correlated Brownian motions (except Sacerdote *et al.* [24], in which several joint densities in a more general setting of diffusion processes were obtained), where 'not available' is denoted as '—'. In the first row (i) means $\mathbb{P}^{(x_1,x_2)}(|\tau_1 - \tau_2| \le t)$, (ii) means $\mathbb{E}^{(0,0)}[(-J_1(\varepsilon_p))(-J_2(\varepsilon_p))]$, and (iii) means $\mathbb{E}^{(0,0)}[(-J_1(\varepsilon_{p_1}))(-J_2(\varepsilon_{p_2}))]$ (we also abbreviate 'arbitrary drifts' to 'a.d.'). Notably, the numerical efficiency of our methods in calculating $\mathbb{P}^{(x_1,x_2)}(\min(\tau_1, \tau_2) \le t)$ and $\mathbb{P}^{(x_1,x_2)}(\tau_1 \le t_1,\ \tau_2 \le t_2)$ for the case of $\mu_1^2 + \mu_2^2 > 0$ is independently demonstrated in Ching *et al.* [6].

	$\mathbb{P}^{(x_1,x_2)}(\min(\tau_1, \tau_2) \le t)$		$\mathbb{P}^{(x_1,x_2)}(\tau_1 \le t_1,\ \tau_2 \le t_2)$		(i)	(ii)	(iii)
	$\mu_1 = \mu_2 = 0$	$\mu_1^2 + \mu_2^2 > 0$	$\mu_1 = \mu_2 = 0$	$\mu_1^2 + \mu_2^2 > 0$			
Spitzer [26]	Integral transform	—	—	—	—	—	—
Iyengar [16]	Analytical expression	—	Joint density	—	—	—	—
He *et al.* [14]	Analytical expression with joint distribution (two-dim. integral)	Analytical expression with joint distribution (two-dim. integral)	—	—	—	—	—
Zhou [28]	Analytical expression	—	—	—	—	—	—
Rogers and Shepp [23]	Laplace transform	—	—	—	—	Analytical expression ($\mu_1 = \mu_2 = 0$) (a.d.)	—
Metzler [20]	Correct typos in [16]	—	Correct typos in [16]	Monte Carlo method	Monte Carlo method (a.d.)	—	—
Sacerdote *et al.* [24]	—	—	Analytical expression of density	Analytical expression of density	—	—	—
This paper	Laplace transform	Laplace transform	Laplace transform	Laplace transform	Laplace transform (a.d.)	Analytical expression (a.d.)	Analytical expression (a.d.)

2. Main results

2.1. Basic ideas

To obtain the required quantities mentioned above, we shall solve the following nonhomogeneous PDE:

$$\frac{1}{2}\sigma_1^2 \frac{\partial^2 u}{\partial x_1^2} + \rho\sigma_1\sigma_2 \frac{\partial^2 u}{\partial x_1 \partial x_2} + \frac{1}{2}\sigma_2^2 \frac{\partial^2 u}{\partial x_2^2} + \mu_1 \frac{\partial u}{\partial x_1} + \mu_2 \frac{\partial u}{\partial x_2} = cu, \qquad x_1, x_2 > 0, \tag{6}$$

with a nonhomogeneous boundary condition

$$u(x_1, x_2)|_{x_1=0} = \mathrm{e}^{-D_2 x_2}, \qquad u(x_1, x_2)|_{x_2=0} = \mathrm{e}^{-D_1 x_1}, \tag{7}$$

and uniform boundedness on the whole domain

$$|u| \leq C \quad \text{(for some constant } C > 1 \text{ not depending on } x_1 \text{ and } x_2). \tag{8}$$

The PDE (6)–(8) is a nonhomogeneous, modified Helmholtz equation in the positive quadrant (or in an infinite wedge, if one switches to polar coordinates and removes the cross correlation term in the PDE, as we shall see shortly). To a large extent, whether one can solve a PDE analytically depends on the boundary conditions. For example, for the above modified Helmholtz equations, the analytical solution is well known if the boundary conditions are on a disk. However, the main difficulty here is that the boundary conditions are on an infinite wedge with an angle, making the PDE difficult to solve analytically.

In the existing literature, there are various numerical schemes available for solving modified Helmholtz equations with some limitations.

- Many of them are performed on a case-by-case basis. For example, the authors in [3] solve the problem when the angle of the wedge is $\pi/4$. The results of [5] and [18] provide fast numerical algorithms, but only on bounded domains.
- None of the results listed above can guarantee that the numerical solution is uniformly bounded as in (8) and, hence, a bona fide Laplace transform (see Theorem 2).

We present two approaches to solve the aforementioned PDE, one by the finite Fourier transform and the other by the Kontorovich–Lebedev transform. On the one hand, the finite Fourier transform is obtained by moving the nonhomogeneous boundary conditions inside the PDE itself (see Lemma 1), from which the nonhomogeneous PDE with homogeneous boundary conditions can be solved by using the finite Fourier transform. On the other hand, the Kontorovich–Lebedev transform is used to match the nonhomogeneous boundary condition exactly, thanks to an algebraic identity; see [29, Equation (C.1)].

After solving the PDE in two ways, several issues remain.

- Is the solution to the PDE unique?
- Do the two approaches yield the same solution?
- Which solution is better?

For the first question, we prove that the solution is unique using a martingale argument; see Theorem 1 below. For the second question, the two approaches aforementioned yield the same unique solution; see Theorem 2 below. For the third question, the finite Fourier transform approach is better in terms of numerical calculation (see Section 3.1) and has broader applicability in some cases (see Remark 2). The Kontorovich–Lebedev transform, on the other hand, is convenient in verifying the uniformly boundedness of solutions; see the proof of the uniform boundedness of u_2 in [29, Lemma 3].

2.2. Removing the boundary conditions

Introduce the polar coordinates r and θ:

$$r = \sqrt{z_1^2 + z_2^2}, \qquad \tan\theta = \frac{z_2}{z_1}, \qquad z_1 = \frac{1}{\sqrt{1-\rho^2}}\left(\frac{x_1}{\sigma_1} - \rho\frac{x_2}{\sigma_2}\right), \qquad z_2 = \frac{x_2}{\sigma_2},$$

and $\alpha \in [0, \pi)$ (note that $x_2 > 0$) defined via

$$\sin\alpha = \sqrt{1-\rho^2}, \qquad \cos\alpha = -\rho. \tag{9}$$

Define the constants a, A and the function G as

$$a \equiv a(c) = \sqrt{2c + \gamma_1^2 + \gamma_2^2}, \qquad \gamma_1 = \frac{\mu_1/\sigma_1 - \rho\mu_2/\sigma_2}{\sqrt{1-\rho^2}}, \qquad \gamma_2 = \frac{\mu_2}{\sigma_2}, \tag{10}$$

$$A \equiv A(c, D_1, D_2) = \sigma_1^2 D_1^2 + 2\rho\sigma_1\sigma_2 D_1 D_2 + \sigma_2^2 D_2^2 - 2\mu_1 D_1 - 2\mu_2 D_2 - 2c,$$
$$G(\theta) := -\gamma_1 \cos\theta - \gamma_2 \sin\theta + D_1\sigma_1 \sin(\alpha - \theta) + D_2\sigma_2 \sin\theta. \tag{11}$$

Lemma 1. (i) (Removing the boundary conditions.) *Any solution, if it exists, to the PDE*

$$\frac{1}{2}\bigg(\frac{\partial^2 k}{\partial r^2} + \frac{1}{r}\frac{\partial k}{\partial r} + \frac{1}{r^2}\frac{\partial^2 k}{\partial \theta^2}\bigg) = \frac{1}{2}a^2 k, \tag{12}$$

with a nonhomogeneous boundary condition on an infinite wedge

$$k(r,\theta)|_{\theta=0} = \mathrm{e}^{-G(0)r}, \qquad k(r,\theta)|_{\theta=\alpha} = \mathrm{e}^{-G(\alpha)r}, \tag{13}$$

is equivalent to a solution to

$$\frac{1}{2}\bigg(\frac{\partial^2 h}{\partial r^2} + \frac{1}{r}\frac{\partial h}{\partial r} + \frac{1}{r^2}\frac{\partial^2 h}{\partial \theta^2}\bigg) = \frac{1}{2}a^2 h - \frac{1}{2}A\mathrm{e}^{-G(\theta)r}, \tag{14}$$

with a homogeneous boundary condition on an infinite wedge

$$h(r,\theta)|_{\theta=0} = 0, \qquad h(r,\theta)|_{\theta=\alpha} = 0, \tag{15}$$

via

$$h(r,\theta) = k(r,\theta) - \mathrm{e}^{-G(\theta)r}. \tag{16}$$

(ii) (Change of variables.) *Any solution to (12) and (13), if it exists, leads to a solution to (6) and (7), i.e.*

$$u(x_1, x_2) = \mathrm{e}^{-(\gamma_1\cos\theta + \gamma_2\sin\theta)r} k(r,\theta).$$

Equivalently, any solution to (14) and (15), if it exists, leads to a solution to (6) and (7), i.e.

$$u(x_1, x_2) = \mathrm{e}^{-(\gamma_1\cos\theta + \gamma_2\sin\theta)r} h(r,\theta) + \mathrm{e}^{-D_1x_1 - D_2x_2}.$$

Proof. See [29]. □

Remark 1. Though simple, (11) and (16) are among the key steps in this paper, from which the removing of the boundary conditions in (15) is made possible, partly because the two boundary conditions in (7) and (13) are both exponential functions and the derivatives of exponential functions are still exponential functions. Not surprisingly, it took the authors some time to find these simple equations.

2.3. Uniqueness and stochastic representation

To find an expression for the unique solution to the PDE problem, we need the following definition and conditions.

Definition 1. Introduce p_1, p_2, and v as $p_1 \equiv p_1(c, D_1, D_2) := \frac{1}{4}\sigma_1^2 D_1^2 - \frac{1}{2}\mu_1 D_1 - \frac{1}{4}\sigma_2^2 D_2^2 + \frac{1}{2}\mu_2 D_2 + \frac{1}{2}c$, $p_2 \equiv p_2(c, D_1, D_2) := \frac{1}{4}\sigma_2^2 D_2^2 - \frac{1}{2}\mu_2 D_2 - \frac{1}{4}\sigma_1^2 D_1^2 + \frac{1}{2}\mu_1 D_1 + \frac{1}{2}c$, and $v \equiv v(c, D_1, D_2) := \frac{1}{4}\sigma_1^2 D_1^2 - \frac{1}{2}\mu_1 D_1 + \frac{1}{4}\sigma_2^2 D_2^2 - \frac{1}{2}\mu_2 D_2 - \frac{1}{2}c$, or, equivalently,

$$c(p_1, p_2) = p_1 + p_2, \qquad D_j(p_j, v) = \frac{\sqrt{\mu_j^2 + 2(p_j + v)\sigma_j^2} + \mu_j}{\sigma_j^2}, \quad j = 1, 2. \tag{17}$$

Note that, for the one-dimensional first-passage time, we have the Laplace transform

$$\mathbb{E}^x(\mathrm{e}^{-p\tau}) = \mathrm{e}^{-((\mu^2+2\sigma^2 p)^{1/2}+\mu)x/\sigma^2}, \qquad x > 0.$$

This is the motivation for D_i.

Condition 1. *We have*

(i) $p_1 + p_2 > 0$ *and*

(ii) $\min(p_1, p_2) + v > 0$ *(so that c, D_1, and D_2 are positive).*

Condition 2. *We have*

(i) $p_1 + p_2 > 0$ *and*

(ii) $\min(p_1, p_2) + v \geq M$, *where*

$$M = \max\biggl(0, \frac{1}{2}\biggl[\biggl(\frac{2(|\gamma_1| + |\gamma_2|)}{\sin\alpha} + 1 - \frac{\mu_1}{\sigma_1}\biggr)^2 - \biggl(\frac{\mu_1}{\sigma_1}\biggr)^2\biggr], \frac{1}{2}\biggl[\biggl(\frac{2(|\gamma_1| + |\gamma_2|)}{\sin\alpha} + 1 - \frac{\mu_2}{\sigma_2}\biggr)^2 - \biggl(\frac{\mu_2}{\sigma_2}\biggr)^2\biggr]\biggr)$$

and α, γ_1, γ_2 are defined in (9) and (10).

There are cases in which Condition 1 holds but Condition 2 does not; for example, take $p_1 = p_2 = v = \frac{1}{2}(M - 1)$. There are also many cases of interest where (p_1, p_2, v) satisfies Condition 2; see Section 2.5.

Theorem 1. (Uniqueness and stochastic representation.) *Suppose that Condition 1 holds. Then any solution to (6)–(8), if it exists, is unique and has the following stochastic representation:*

$$u(x_1, x_2) = \mathbb{E}^{(x_1,x_2)}[\mathrm{e}^{-p_1\tau_1 - p_2\tau_2 - v|\tau_2-\tau_1|}].$$

Proof. See [29]. □

2.4. Existence and analytical solutions

Theorem 2. (Existence and the analytical solution.) *Suppose that Condition 2 holds (and, hence, Condition 1 also holds). Then the unique solution u_1 to the PDE problem (6)–(8) is given by*

$$u_1(x_1, x_2) := \mathrm{e}^{-(\gamma_1\cos\theta+\gamma_2\sin\theta)r}\biggl(\sum_{n=1}^{\infty}\sqrt{\frac{2}{\alpha}}\sin(\nu_n\theta)U_n(r)\biggr) + \mathrm{e}^{-D_1x_1-D_2x_2}. \tag{18}$$

In addition, another representation of $u_1(x_1, x_2)$ is given by

$$u_1(x_1, x_2) = u_2(x_1, x_2) : = \mathrm{e}^{-(\gamma_1\cos\theta+\gamma_2\sin\theta)r}k(r, \theta).$$

Here,

$$\nu_n = \frac{n\pi}{\alpha} \geq n, \qquad H_1 = G(0) = -\gamma_1 + D_1\sigma_1\sin\alpha,$$
$$H_2 = G(\alpha) = -\gamma_1\cos\alpha - \gamma_2\sin\alpha + D_2\sigma_2\sin\alpha,$$

Also,

$$U_n(r) = \frac{1}{2}A(c, D_1, D_2)\int_{\eta=0}^{\alpha}\sqrt{\frac{2}{\alpha}}\sin(\nu_n\eta)\bigg[K_{\nu_n}(ar)\int_{l=0}^{r}\mathrm{e}^{-G(\eta)l}lI_{\nu_n}(al)\,\mathrm{d}l + I_{\nu_n}(ar)\int_{l=r}^{\infty}\mathrm{e}^{-G(\eta)l}lK_{\nu_n}(al)\,\mathrm{d}l\bigg]\,\mathrm{d}\eta,$$

$$k(r,\theta) = \frac{2}{\pi}\int_0^{\infty}\frac{K_{\mathrm{i}\nu}(ar)}{\sinh(\alpha\nu)}[\cosh(\beta_1\nu)\sinh((\alpha-\theta)\nu) + \cosh(\beta_2\nu)\sinh(\theta\nu)]\,\mathrm{d}\nu,$$

$$\beta_j(c) = \arccos\bigg(\frac{H_j}{a(c)}\bigg) = -\mathrm{i}\log\bigg(\frac{H_j}{a(c)} + \mathrm{i}\sqrt{1-\frac{H_j^2}{a(c)^2}}\bigg), \qquad j = 1, 2,$$

and $I_\nu(\cdot)$ and $K_\nu(\cdot)$ are modified Bessel functions with order ν of the first kind and the second kind, respectively. Note that H_i depends on D_i, which in turns depends on p_1, p_2, and v via (17).

Proof. See [29]. □

For the two representations in Theorem 2, u_2 is easier for proving certain theoretical properties; for example, it is easier to show the uniform boundedness of u_2 (see [29, Lemma 3]), while u_1 is better in numerical calculation. More precisely, for u_1 by the finite Fourier transform, we can compute the double integrals in $U_n(r)$ easily by using the MATLAB® function 'quadgk', based on an adaptive Gauss–Kronrod quadrature; see [25]. However, for u_2 we need to be able to calculate the modified Bessel function of the second kind with both degrees of freedom and the argument being complex, because the Laplace inversion algorithm requires the function evaluated at complex values.

This leads to difficulties in implementing the expression u_2.

- Although there are ways of computing $K_{ix}(ar)$ or the Kontorovich–Lebedev transform directly (see, for example, [9]), it seems that none of the authors has dealt with the case when the argument of $K_{ix}(ar)$ is complex.
- There are also a few asymptotic expansions of $K_{ix}(ar)$, but numerical procedures based on these formulae do not seem stable in our numerical experiments. We find that it is better to use the following definition of $K_{\mathrm{i}\nu}(\cdot)$, which is well defined and numerically stable when the argument of $K_{\mathrm{i}\nu}(ar)$ is complex: $K_{\mathrm{i}\nu}(ar) = \int_0^\infty \mathrm{e}^{-ar\cosh(t)}\cos(\nu t)\,\mathrm{d}t$.

Hence, the expression in u_2 again becomes a double infinite integral, one with t and the other with ν. The evaluation of the double integral in u_2 takes longer than that in u_1, partly due to the combination of exponential, cosh, and the oscillation function cos in the integrand of $K_{\mathrm{i}\nu}(ar)$.

2.5. Special cases

Theorem 2 above reduces to several special cases with different choices of parameters.

Case 1. When $v = 0$ and $\min(p_1, p_2) \geq M$. Then $p_1 + p_2 > 0$, $\min(p_1, p_2) + v \geq M$ (Condition 2 holds) and the special case is

$$L(x_1, x_2) = \mathbb{E}^{(x_1,x_2)}[\mathrm{e}^{-p_1\tau_1 - p_2\tau_2}]. \tag{19}$$

In what follows, we let L_1 be the expression by u_1 in Theorem 2 (using the finite Fourier transform) and L_2 the expression by u_2 (using the Kontorovich–Lebedev transform).

Case 2. When $p_1 = p_2 = \frac{1}{2}q$, $v = s - \frac{1}{2}q$, *and* $q > 0$, $s \geq M$. Then $p_1 + p_2 = q > 0$, $\min(p_1, p_2) + v = s \geq M$ (Condition 2 holds), and $p_1\tau_1 + p_2\tau_2 + v|\tau_1 - \tau_2| = \frac{1}{2}q(2\tau^* + |\tau_1 - \tau_2|) + (s - \frac{1}{2}q)|\tau_1 - \tau_2| = q\tau^* + s|\tau_1 - \tau_2|$, and the special case is

$$T(x_1, x_2) = \mathbb{E}^{(x_1,x_2)}[\mathrm{e}^{-q\tau^* - s|\tau_2 - \tau_1|}]. \tag{20}$$

In what follows, we let T_1 be the expression by u_1 in Theorem 2 (using the finite Fourier transform) and T_2 the expression by u_2 (using the Kontorovich–Lebedev transform).

Case 3. Let $p_1 = p_2 = v = \frac{1}{2}p$ *and* $p \geq M$. Then $p_1 + p_2 = p > 0$, $\min(p_1, p_2) + v = p \geq M$ (Condition 2 holds), and $p_1\tau_1 + p_2\tau_2 + v|\tau_1 - \tau_2| = \frac{1}{2}p(2\tau^* + |\tau_1 - \tau_2|) + \frac{1}{2}p|\tau_1 - \tau_2| = \frac{1}{2}p(2\tilde{\tau}) = p\tilde{\tau}$, where $\tilde{\tau} := \max(\tau_1, \tau_2)$. In particular,

$$\mathbb{E}^{(x_1,x_2)}[\mathrm{e}^{-p\tilde{\tau}}] = \frac{2}{\pi}\mathrm{e}^{-(\gamma_1\cos\theta + \gamma_2\sin\theta)r}\int_{\nu=0}^{\infty}\frac{K_{\mathrm{i}\nu}(ar)}{\sinh(\alpha\nu)}[\cosh(\beta_1\nu)\sinh((\alpha-\eta)\nu) + \cosh(\beta_2\nu)\sinh(\eta\nu)]\,\mathrm{d}\nu. \tag{21}$$

In the special case of $\mu_1 = \mu_2 = 0$ and $\sigma_1 = \sigma_2 = 1$, the expression for $\mathbb{E}^{(x_1,x_2)}(\mathrm{e}^{-p\tilde{\tau}})$ simplifies to

$$\begin{aligned}\mathbb{E}^{(x_1,x_2)}(\mathrm{e}^{-p\tilde{\tau}}) &= \frac{2}{\pi}\int_0^{\infty}\frac{K_{\mathrm{i}\nu}(\sqrt{2p}r)}{\sinh(\alpha\nu)}\biggl[\cosh\biggl(\biggl(\frac{\pi}{2} - \alpha\biggr)\nu\biggr)(\sinh((\alpha-\theta)\nu) + \sinh(\theta\nu))\biggr]\,\mathrm{d}\nu \\ &= \frac{2}{\pi}\int_0^{\infty}\frac{K_{\mathrm{i}\nu}(\sqrt{2p}r)}{\cosh(\alpha\nu/2)}\biggl[\cosh\biggl(\biggl(\frac{\pi}{2} - \alpha\biggr)\nu\biggr)\cosh\biggl(\frac{\alpha\nu}{2} - \theta\nu\biggr)\biggr]\,\mathrm{d}\nu,\end{aligned}$$

where in the second equality we have made use of the following two identities: $\sinh((\alpha - \theta)\nu) + \sinh(\theta\nu) = 2\sin(\alpha\nu/2)\cosh(\alpha\nu/2 - \theta\nu)$ and $\sinh(\alpha\nu) = 2\sinh(\alpha\nu/2)\cosh(\alpha\nu/2)$.

Case 4. The special case $\tilde{L}(x_1, x_2) = \mathbb{E}^{(x_1,x_2)}(\mathrm{e}^{-p\tau^*})$. This can be expressed as

$$\mathbb{E}^{(x_1,x_2)}(\mathrm{e}^{-p\tau^*}) = \mathbb{E}^{x_1}(\mathrm{e}^{-p\tau_1}) + \mathbb{E}^{x_2}(\mathrm{e}^{-p\tau_2}) - \mathbb{E}^{(x_1,x_2)}(\mathrm{e}^{-p\tilde{\tau}}). \tag{22}$$

In what follows, we let $\tilde{L}_1$ be the expression by u_1 in Theorem 2 (using the finite Fourier transform) and $\tilde{L}_2$ the expression by u_2 (using the Kontorovich–Lebedev transform).

Remark 2. An advantage of the finite Fourier transform can also be seen by comparing the expressions of T_1 and T_2 in (20). In particular, T_2 is not well defined when $\mu_1 = \mu_2 = 0$ and $q \downarrow 0$. To see that, note that, by definition, $a(c) = a(q) = (2q + \gamma_1^2 + \gamma_2^2)^{1/2} \downarrow 0$ in this case, which implies that β_1, β_2 become $\mathrm{i}\cdot\infty$ while $\cosh(\mathrm{i}\cdot\infty)$ is not well defined. To the contrary, T_1 by the finite Fourier transform is well defined for arbitrary γ_1 and γ_2 when $q \downarrow 0$.

3. Numerical computation of $\mathbb{P}(\tau_1 \leq t_1,\ \tau_2 \leq t_2)$ and application to default correlation

3.1. Numerical results

To obtain the joint probability distribution of τ_1 and τ_2, numerical inversion of the Laplace transform is applied on both the formulae of $L_1(x_1, x_2)$ and $L_2(x_1, x_2)$ in (19), which are special cases of u_1 and u_2 in Theorem 2, respectively. The double Laplace inversion formula is given in [4] (which extends [1]). Note that here the technical condition in Section 2.5 that p_1 and p_2 are sufficiently large (related to Condition 2 and [29, Lemma 2]) does not impose obstacles in devising the inversion algorithm. This is because the double inversion algorithm evaluates the joint Laplace transform at complex values with large real parts; see [4] for more detail in this regard.

To obtain a benchmark, the joint probability distribution function is calculated using Monte Carlo simulation. We use 2000, 4000, and 8000 time-discretization grids, and perform the

Richardson extrapolation of order $\frac{1}{2}$ to reduce discretization bias. For each probability, 100 000 two-dimensional Brownian paths are simulated.

One can see from Table 2 that probabilities obtained from inverting joint Laplace transforms align well with the benchmark for various combinations of correlations ($\rho = 0.2, 0.5, 0.8$), drifts ($\mu_1 = 0.2, -0.2, \mu_2 = 0.15, -0.15$), and volatilities ($\sigma_1 = \sigma_2 = 0.55, 0.2$).

TABLE 2: We obtain $\mathbb{P}^{(x_1,x_2)}(\tau_1 \le t_1,\ \tau_2 \le t_2)$ via the inversion of the joint Laplace transform (column L_1 (FT) and by the finite Fourier transform, and column L_2 (KL) by the Kontorovich–Lebedev transform), compared with those obtained by the Monte Carlo simulation (column MC) and by Sacerdote *et al.* [24, Equation (22)] (column STZ), when $t_1 = 0.3$, $t_2 = 0.5$ with various combinations of correlations ($\rho = 0.2, 0.5, 0.8$), drifts ($\mu_1 = 0.2, -0.2, \mu_2 = 0.15, -0.15$), and volatilities ($\sigma_1 = \sigma_2 = 0.55, 0.2$). Here, the probabilities in MC are computed using 100 000 Brownian paths with 2000, 4000, and 8000 time-discretization grids. The Richardson extrapolation of order $\frac{1}{2}$ is exploited to reduce discretization bias in the simulation. Starting points are set to be $x_1 = x_2 = \ln(1.2) = 0.1823$. The CPU time is in seconds. Each number in parenthesis in the column of MC is the standard deviation of the Monte Carlo simulation.

	High volatilities: $\sigma_1 = \sigma_2 = 0.55$									
	μ_1	μ_2	L_1 (FT)	CPU time	L_2 (KL)	CPU time	MC (std)	CPU time	STZ	CPU time
$\rho = 0.2$	0.2	0.15	0.3055	115.6	0.3056	519.5	0.3053 (0.0015)	22240.7	0.3053	3089.2
	−0.2	0.15	0.3804	115.3	0.3809	514.6	0.3823 (0.0015)	21847.3	0.3805	3107.1
	0.2	−0.15	0.3583	115.3	0.3676	512.2	0.3579 (0.0016)	21344.4	0.3572	3087.4
	−0.2	−0.15	0.4480	115.1	0.4483	515.8	0.4486 (0.0016)	21397.7	0.4479	3092.9
$\rho = 0.5$	0.2	0.15	0.3489	112.5	0.3498	515.5	0.3485 (0.0015)	21381.4	0.3496	3056.1
	−0.2	0.15	0.4243	112.2	0.4246	513.7	0.4238 (0.0015)	21592.5	0.4239	3065.5
	0.2	−0.15	0.3978	112.0	0.3958	515.4	0.3966 (0.0016)	21626.3	0.3999	3062.0
	−0.2	−0.15	0.4860	112.0	0.4875	512.8	0.4870 (0.0015)	20387.5	0.4885	3060.4
$\rho = 0.8$	0.2	0.15	0.4055	116.1	0.4054	520.5	0.4041 (0.0016)	21580.6	0.4036	3599.8
	−0.2	0.15	0.4789	115.0	0.4801	520.7	0.4796 (0.0016)	21775.4	0.4783	3585.5
	0.2	−0.15	0.4409	117.6	0.4408	519.5	0.4408 (0.0016)	20526.6	0.4405	3576.3
	−0.2	−0.15	0.5353	115.3	0.5362	527.3	0.5354 (0.0016)	21487.6	0.5355	3597.8
	Low volatilities: $\sigma_1 = \sigma_2 = 0.2$									
	μ_1	μ_2	L_1 (FT)	CPU time	L_2 (KL)	CPU time	MC (std)	CPU time	STZ	CPU time
$\rho = 0.2$	0.2	0.15	0.0059	115.9	0.0058	472.5	0.0061 (0.0004)	18100.5	0.0057	3134.0
	−0.2	0.15	0.0288	115.0	0.0287	490.5	0.0285 (0.0006)	17101.2	0.0283	3116.1
	0.2	−0.15	0.0195	114.9	0.0198	464.4	0.0192 (0.0007)	17350.2	0.0191	3115.8
	−0.2	−0.15	0.0960	114.8	0.0954	490.4	0.0951 (0.0005)	15830.4	0.0944	3122.3
$\rho = 0.5$	0.2	0.15	0.0122	127.8	0.0125	495.8	0.0122 (0.0007)	17223.5	0.0119	3061.1
	−0.2	0.15	0.0462	127.6	0.0463	487.1	0.0460 (0.0008)	16235.3	0.0450	3063.8
	0.2	−0.15	0.0258	124.5	0.0261	488.6	0.0255 (0.0005)	16485.0	0.0250	3061.5
	−0.2	−0.15	0.1297	122.5	0.1298	480.6	0.1292 (0.0006)	14997.9	0.1296	3081.1
$\rho = 0.8$	0.2	0.15	0.0224	122.6	0.0224	491.3	0.0226 (0.0007)	15840.5	0.0216	3645.6
	−0.2	0.15	0.0679	122.7	0.0685	498.3	0.0679 (0.0006)	14967.5	0.0670	3769.9
	0.2	−0.15	0.0330	123.1	0.0335	493.5	0.0334 (0.0007)	15204.0	0.0338	3803.6
	−0.2	−0.15	0.1667	122.2	0.1668	503.9	0.1660 (0.0008)	13601.6	0.1666	3588.6

However, the differences for the processor time (CPU) are significant. Given a set of parameters, it typically takes less than 2 minutes for the algorithm using L_1 to compute one probability and 7–9 minutes for the algorithm using L_2, while Monte Carlo simulation with the Richardson extrapolation usually takes 4–6 hours.

We also compare the accuracy and efficiency of our method to the results in [24], where the joint density function of (τ_1, τ_2) (Equation (22) therein) is obtained via an interesting conditional density argument and a solution of a two-dimensional Kolmogorov forward equation. To obtain the joint probability function from the joint density in [24], one can, in principle, perform a double numerical summation, i.e.

$$\mathbb{P}(\tau_1 \le t_1,\ \tau_2 \le t_2) = \int_{s_1=0}^{t_1} \int_{s_2=0}^{t_2} f_{\tau_1,\tau_2}(s_1, s_2)\,\mathrm{d}s_1\,\mathrm{d}s_2 \approx \sum_{m=1}^{N} \sum_{n=1}^{N} f_{\tau_1,\tau_2}\biggl(\frac{mt_1}{N}, \frac{nt_2}{N}\biggr)\frac{t_1 t_2}{N^2},$$

where f_{τ_1,τ_2} is the joint density function. However, one challenge of implementing the double summation is that the joint density function $f_{\tau_1,\tau_2}(s_1, s_2) \to \infty$ when $s_1 \to s_2$ and $\rho > 0$. Therefore, whenever $mt_1/N = nt_2/N$, we replace $f_{\tau_1,\tau_2}(mt_1/N, nt_2/N)$ by $f_{\tau_1,\tau_2}(mt_1/N, nt_2/N + \delta)$, where δ is 10^{-5} in the numerical experiment. To achieve comparable accuracy, $N = 120$ is used (and $n = 10$ is used to compute the infinite sum for G_{ij} in [24, Equation (2.2)]). The last two columns in Table 2 show that our numerical results match those produced by [24, Equation (22)], while our method (via either the finite Fourier transform or the Kontorovich–Lebedev transform) is much faster, partly because our formula computes the probability via the Laplace transform, thus avoiding the singularity of the density.

Furthermore, the steps that lead to the solution in [24] are not entirely rigorous. For example, the PDE problem involves the Dirac delta function in the initial condition and thus it is not immediately clear whether the equation has a unique solution via bounded martingale arguments. Even when there is a unique solution it is not clear whether that unique solution admits the required stochastic representation. In this paper we attempt to deal with these issues rigorously. For example, after showing the uniqueness for uniformly bounded solutions, via the stochastic representation using a martingale argument in Theorem 1, we put significant effort into proving that the two solutions u_1 and u_2 in Theorem 2 are all uniformly bounded and are the same.

3.2. Application to default correlation

In [28], default correlation is defined as

$$\begin{aligned}\operatorname{corr}(\mathbf{1}(\tau_1 \le t), \mathbf{1}(\tau_2 \le t)) &:= \frac{\mathbb{E}^{(x_1,x_2)}[\mathbf{1}(\tau_1 \le t)\,\mathbf{1}(\tau_2 \le t)] - \mathbb{E}^{x_1}[\mathbf{1}(\tau_1 \le t)]\mathbb{E}^{x_2}[\mathbf{1}(\tau_2 \le t)]}{\sqrt{\operatorname{var}(\mathbf{1}(\tau_1 \le t))\operatorname{var}(\mathbf{1}(\tau_2 \le t))}} \\ &= \frac{\mathbb{P}^{(x_1,x_2)}(\tau_1 \le t \text{ and } \tau_2 \le t) - \mathbb{P}^{x_1}(\tau_1 \le t)\mathbb{P}^{x_2}(\tau_2 \le t)}{\sqrt{\mathbb{P}^{x_1}(\tau_1 \le t)(1 - \mathbb{P}^{x_1}(\tau_1 \le t))\mathbb{P}^{x_2}(\tau_2 \le t)(1 - \mathbb{P}^{x_2}(\tau_2 \le t))}},\end{aligned}$$

where $\mathbf{1}$ is the indicator function. In [28], the above was computed in the special case of $\mu_1 = \mu_2 = 0$. In this section we extend this study by checking whether the correlation will change when μ_1 and μ_2 are nonzero. Also, we consider default correlation for τ_1, τ_2 in different horizons, where $t_1 \ne t_2$ in the following:

$$\begin{aligned}&\operatorname{corr}(\mathbf{1}(\tau_1 \le t_1), \mathbf{1}(\tau_2 \le t_2)) \\ &\quad = \frac{\mathbb{P}^{(x_1,x_2)}(\tau_1 \le t_1 \text{ and } \tau_2 \le t_2) - \mathbb{P}^{x_1}(\tau_1 \le t_1)\mathbb{P}^{x_2}(\tau_2 \le t_2)}{\sqrt{\mathbb{P}^{x_1}(\tau_1 \le t_1)(1 - \mathbb{P}^{x_1}(\tau_1 \le t_2))\mathbb{P}^{x_2}(\tau_2 \le t_2)(1 - \mathbb{P}^{x_2}(\tau_2 \le t_2))}}.\end{aligned}$$

The results are summarized in Tables 3 and 4. It appears that nonzero drifts can have a significant impact on default correlations.

TABLE 3: Default correlation $\operatorname{corr}(\mathbf{1}(\tau_1 \le t), \mathbf{1}(\tau_2 \le t))$ (in percent) with different combinations of drifts and maturities. Parameters used are the same as in [28]. The numbers in bold are also computed in [28].

$x_1 = x_2 = \ln(5)$, $\sigma_1 = \sigma_2 = 30\%$, and $\rho = 40\%$					
	$t_1 = 2$				
	$t_2 = 1$	$t_2 = 2$	$t_2 = 3$	$t_3 = 4$	$t_2 = 5$
$\mu_1 = \mu_2 = 0$	0.0198%	1.1723 %	1.3466%	1.2564%	1.0924%
$\mu_1 = \mu_2 = 30\%$	0.0012%	0.0683%	0.0643%	0.0548%	0.0482%
$\mu_1 = \mu_2 = -30\%$	0.1699%	8.4898%	9.2264%	7.1381%	4.4529%
	$t_1 = 4$				
	$t_2 = 1$	$t_2 = 2$	$t_2 = 3$	$t_3 = 4$	$t_2 = 5$
$\mu_1 = \mu_2 = 0$	0.0026%	1.2564%	4.0316%	**6.5837%**	7.0248%
$\mu_1 = \mu_2 = 30\%$	0.0003%	0.0548%	0.1783%	0.2715%	0.2748%
$\mu_1 = \mu_2 = -30\%$	−0.1495%	7.1381%	18.2286%	24.6885%	22.9000%
	$t_1 = 5$				
	$t_2 = 1$	$t_2 = 2$	$t_2 = 3$	$t_3 = 4$	$t_2 = 5$
$\mu_1 = \mu_2 = 0$	0.0001%	1.0924%	3.9462%	7.0248%	**9.1974%**
$\mu_1 = \mu_2 = 30\%$	0.0003%	0.0482%	0.1643%	0.2748%	0.3328%
$\mu_1 = \mu_2 = -30\%$	−0.2713%	4.4529%	15.8324%	22.9000%	25.8568%

TABLE 4: Default correlation $\operatorname{corr}(\mathbf{1}(\tau_1 \le t), \mathbf{1}(\tau_2 \le t))$ (in percent) with different combinations of drifts and maturities.

$x_1 = x_2 = \ln(1.2)$, $\sigma_1 = \sigma_2 = 55\%$, and $\rho = 50\%$					
	$t_1 = 2$				
	$t_2 = 1$	$t_2 = 2$	$t_2 = 3$	$t_3 = 4$	$t_2 = 5$
$\mu_1 = \mu_2 = 0$	24.8%	25.5%	24.0%	22.7%	21.7%
$\mu_1 = \mu_2 = 30\%$	28.2%	28.6%	28.1%	27.7%	27.5%
$\mu_1 = \mu_2 = -30\%$	19.0%	19.8%	16.7%	14.3%	12.6%
	$t_1 = 4$				
	$t_2 = 1$	$t_2 = 2$	$t_2 = 3$	$t_3 = 4$	$t_2 = 5$
$\mu_1 = \mu_2 = 0$	20.8%	22.7%	23.2%	22.9%	22.3%
$\mu_1 = \mu_2 = 30\%$	26.8%	27.7%	27.9%	27.8%	27.7%
$\mu_1 = \mu_2 = -30\%$	11.9%	14.3%	14.9%	14.3%	12.8%
	$t_1 = 5$				
	$t_2 = 1$	$t_2 = 2$	$t_2 = 3$	$t_3 = 4$	$t_2 = 5$
$\mu_1 = \mu_2 = 0$	19.7%	21.7%	22.1%	22.3%	22.1%
$\mu_1 = \mu_2 = 30\%$	26.5%	27.5%	27.7%	27.7%	27.6%
$\mu_1 = \mu_2 = -30\%$	10.0%	12.6%	12.5%	12.8%	12.5%

4. The density of $|\tau_2 - \tau_1|$

Suppose that $s \geq M$ such that (20) holds. Then $q \downarrow 0$ yields the Laplace transform of $|\tau_1 - \tau_2|$ with $\tau_1, \tau_2 < \infty$, i.e.

$$\begin{aligned}&\mathbb{E}^{(x_1,x_2)}(\mathrm{e}^{-s|\tau_2-\tau_1|}\,\mathbf{1}(\tau_1, \tau_2 < \infty))\\&\quad = \mathrm{e}^{-(\gamma_1\cos\theta+\gamma_2\sin\theta)r}\Bigg(\sum_{n=1}^{\infty}\sqrt{\frac{2}{\alpha}}\sin(\nu_n\theta)V_n(r)\Bigg) + \mathrm{e}^{-D_1(0,s)x_1-D_2(0,s)x_2},\end{aligned} \tag{23}$$

where

$$\begin{aligned}V_n(r) &= (2s + \rho\sigma_1\sigma_2 D_1(0,s)D_2(0,s))\\&\quad\times\int_{\eta=0}^{\alpha}\sqrt{\frac{2}{\alpha}}\sin(\nu_n\eta)\bigg[K_{\nu_n}(a(0)r)\int_{l=0}^{r}\mathrm{e}^{-G(\eta)l}\,l\,I_{\nu_n}(a(0)l)\,\mathrm{d}l\\&\qquad\qquad + I_{\nu_n}(a(0)r)\int_{l=r}^{\infty}\mathrm{e}^{-G(\eta)l}\,l\,K_{\nu_n}(a(0)l)\,\mathrm{d}l\bigg]\,\mathrm{d}\eta,\end{aligned}$$

and all other parameters and functions are defined in Definition 1, (9), and (10). When $\mu_1 = \mu_2 = 0$, $a(0) = 0$ and the modified Helmholtz equation degenerates to a Helmholtz equation;

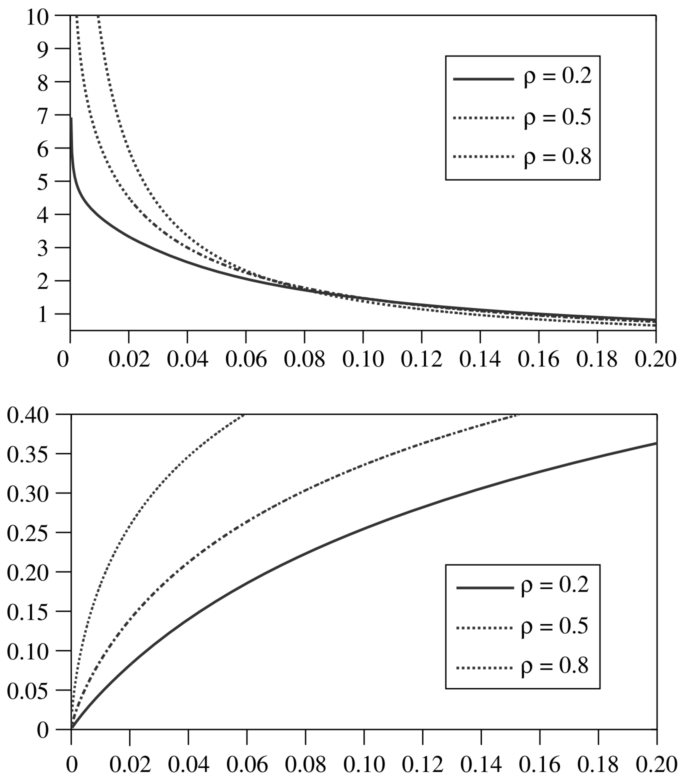

FIGURE 1: The distribution function (*upper*) and density (*lower*) of $|\tau_1 - \tau_2|$ when $\rho = 0.2$, 0.5, and 0.8. We perform numerical Laplace inversion on (23). The correlated zero-drifted Brownian motion starts at $x_1 = x_2 = \log(1.2) = 0.1823$. It can be seen that numerically all three distribution functions tend to 0 as $t \to 0$, while all three density functions seem to tend to ∞ as $t \to 0$. This is proved rigorously in Theorem 3.

as a result, in this case the expression of $V_n(r)$ takes a similar form but no special function is involved, i.e.

$$V_n(r) = \frac{2s + 2\rho s}{\nu_n} \int_{\eta=0}^{\alpha} \sqrt{\frac{2}{\alpha}} \sin(\nu_n \eta) \bigg[\int_{l=0}^{r} \mathrm{e}^{-G(\eta)l} l \left(\frac{l}{r}\right)^{\nu_n} \mathrm{d}l + \int_{l=r}^{\infty} \mathrm{e}^{-G(\eta)l} l \left(\frac{r}{l}\right)^{\nu_n} \mathrm{d}l \bigg] \mathrm{d}\eta.$$

Numerical inversion of (23) yields the distribution function $\mathbb{P}^{(x_1,x_2)}(|\tau_1 - \tau_2| \le t,\ \tau_1, \tau_2 < \infty)$ and the density functions $f_{|\tau_1-\tau_2|}(t)\,\mathrm{d}t := \mathbb{P}^{(x_1,x_2)}(|\tau_1 - \tau_2| \in \mathrm{d}t,\ \tau_1, \tau_2 < \infty)$; see Figure 1.

Theorem 3. *For arbitrary drifts μ_1 and μ_2,*

(i) $\mathbb{P}^{(x_1,x_2)}(\tau_1 = \tau_2,\ \tau_1, \tau_2 < \infty) = 0$ *for any $\rho \in (-1, 1)$;*

(ii) $f_{|\tau_1-\tau_2|}(0+) = \infty$ *if and only if $\rho > 0$.*

Thus, near 0*, the distribution function always tends to* 0 *and the density function may tend to* ∞.

Proof. See [29]. □

5. A class of bivariate exponential distributions

In this section we point out that special cases of solutions in Section 2.5 lead to a class of bivariate exponential distributions (BVEs). To obtain some insight, we first review the first-passage time of the Brownian motion problem in the one-dimensional case. Let ε_p be an exponential random variable with rate p, independent of the Brownian motion $X(t)$. Furthermore, let $J(t) = \min_{0\le s\le t} X(s)$. Then, for $x > 0$, the Laplace transform of the one-dimensional first-passage time is

$$\begin{aligned}
\mathbb{E}^x(\mathrm{e}^{-p\tau}) &= \int_0^{\infty} \mathrm{e}^{-pt}\,\mathrm{d}\mathbb{P}^x(\tau \le t) \\
&= \bigg([\mathrm{e}^{-pt}\mathbb{P}^x(\tau \le t)]|_{t=0}^{\infty} + \int_0^{\infty} p\mathrm{e}^{-pt}\mathbb{P}^x(\tau \le t)\,\mathrm{d}t \bigg) \\
&= \int_0^{\infty} p\mathrm{e}^{-pt}\mathbb{P}^x(-J(t) \ge 0)\,\mathrm{d}t \\
&= \int_0^{\infty} p\mathrm{e}^{-pt}\mathbb{P}^0(-J(t) \ge x)\,\mathrm{d}t \\
&= \mathbb{P}^0(-J(\varepsilon_p) \ge x).
\end{aligned}$$

That is, using the standard result of the one-dimensional first-passage time problem, we are able to show that $\mathbb{P}^0(-J(\varepsilon_p) \ge x) = \mathbb{E}^x(\mathrm{e}^{-p\tau}) = \mathrm{e}^{-((\mu^2+2\sigma^2 p)^{1/2}+\mu)x/\sigma^2}$, $x > 0$. The above implies that starting from 0, $-J(\varepsilon_p)$ is exponentially distributed. Thus, the two-dimensional minimums lead to BVEs.

5.1. Two joint probabilities

There are various definitions of BVEs, depending on features that are desired. The following three features receive most attention:

(i) marginal distributions are exponential;

(ii) absolutely continuous with respect to the Lebesgue measure in $\mathbb{R}^2$;

(iii) the memoryless property holds; namely, for any $x_0, x, y_0, y > 0$,

$$\mathbb{P}(\mathcal{E}_1 > x_0 + x,\ \mathcal{E}_2 > y_0 + y) = \mathbb{P}(\mathcal{E}_1 > x,\ \mathcal{E}_2 > y)\mathbb{P}(\mathcal{E}_1 > x_0,\ \mathcal{E}_2 > y_0).$$

For any BVE with all (i), (ii), and (iii), the two exponential random variables must be independent (see [19]). For more discussion of BVEs; see, for example, [7], [8], [11], and [19].

Example 1. For $x_1, x_2 > 0$ and independent exponential random variables $\varepsilon_{p_1}, \varepsilon_{p_2}$ independent of the Brownian motions, we have

$$\begin{aligned} L(x_1, x_2) &= \mathbb{E}^{(x_1,x_2)}(\mathrm{e}^{-p_1\tau_1 - p_2\tau_2}) \\ &= \int_0^\infty \int_0^\infty p_1 p_2 \mathrm{e}^{-p_1 t_1 - p_2 t_2} \mathbb{P}^{(x_1,x_2)}(\tau_1 \le t_1, \tau_2 \le t_2)\,\mathrm{d}t_1\,\mathrm{d}t_2 \\ &= \int_0^\infty \int_0^\infty p_1 p_2 \mathrm{e}^{-p_1 t_1 - p_2 t_2} \mathbb{P}^{(0,0)}(-J_1(t_1) \ge x_1, -J_2(t_2) \ge x_2)\,\mathrm{d}t_1\,\mathrm{d}t_2 \\ &= \mathbb{P}^{(0,0)}(-J_1(\varepsilon_{p_1}) \ge x_1, -J_2(\varepsilon_{p_2}) \ge x_2), \end{aligned} \tag{24}$$

which can be computed via (19).

Since for each $i = 1, 2$, $-J_i(\varepsilon_{p_i})$ is an exponential random variable, the last term in (24) is then the joint survival function of some BVE. Clearly, $(-J_1(\varepsilon_{p_1}), -J_2(\varepsilon_{p_2}))$ satisfies (i). Moreover, (ii) is also satisfied, since $L(x_1, x_2)$ is by definition twice differentiable and, hence, continuous in (x_1, x_2). Thus, $(-J_1(\varepsilon_{p_1}), -J_2(\varepsilon_{p_2}))$ does not have the memoryless property of (iii), unless $\rho = 0$ and $J_1(\epsilon_{p_1})$ is independent of $J_2(\epsilon_{p_2})$.

Example 2. Stopping at the same exponential variable ε_p independent of the Brownian motions, $(-J_1(\varepsilon_p), -J_2(\varepsilon_p))$ is also a BVE. From (22), the joint survival function of $(-J_1(\varepsilon_p), -J_2(\varepsilon_p))$ is given by

$$\begin{aligned} \mathbb{E}^{(x_1,x_2)}(\mathrm{e}^{-p\tilde{\tau}}) &= \int_0^\infty p\mathrm{e}^{-pt} \mathbb{P}^{(x_1,x_2)}(\tau_1 \le t, \tau_2 \le t)\,\mathrm{d}t \\ &= \int_0^\infty p\mathrm{e}^{-pt} \mathbb{P}^{(0,0)}(-J_1(t) \ge x_1, -J_2(t) \ge x_2)\,\mathrm{d}t \\ &= \mathbb{P}^{(0,0)}(-J_1(\varepsilon_p) \ge x_1, -J_2(\varepsilon_p) \ge x_2), \end{aligned}$$

which can be computed via (21).

Remark 3. Even when $\rho = 0$, $-J_1(\varepsilon_p)$ is not independent of $-J_2(\varepsilon_p)$, since the same ε_p is shared. Hence, the joint distribution of $(-J_1(\varepsilon_p), -J_2(\varepsilon_p))$ is different from that of $(-J_1(\varepsilon_{p_1}), -J_2(\varepsilon_{p_2}))$.

5.2. Two joint moments

A closed-form expression for $\mathbb{E}^{(0,0)}\,[(-J_1(\varepsilon_p))(-J_2(\varepsilon_p))]$ is given in [23] when the underlying correlated Brownian motions have zero drifts. In this subsection, we first generalize the approach of [23] to the case when $(X_1(t), X_2(t))$ has arbitrary drifts; see the first part of Theorem 4. Then we provide a characterization of $\mathbb{E}^{(0,0)}[(-J_1(\varepsilon_{p_1}))(-J_2(\varepsilon_{p_2}))]$ in the case of drifted Brownian motion, where p_1 and p_2 may not be the same; see the second part of Theorem 4.

We first introduce some notation. Let $\Gamma(\cdot)$ be the gamma function, $P_{\nu}^{-\mu}(\cdot)$ the Legendre function (for definition of Legendre function, see, for example, [22, Chapter 8]), and

$$b(\eta, c) := \frac{\gamma_1 \cos(\eta) + \gamma_2 \sin(\eta)}{a(c)},$$
$$Q(\eta, c) := \begin{cases} \log(b(\eta, c) + \sqrt{b(\eta, c)^2 - 1}) & \text{when } b(\eta, c) \in [1, \infty), \\ \mathrm{i} \arccos(b(\eta, c)) & \text{when } b(\eta, c) \in [-1, 1). \end{cases}$$

Since $a(c) = (2c + \gamma_1^2 + \gamma_2^2)^{1/2} \uparrow \infty$ and $b(\eta, c) \to 0$ as $c \uparrow \infty$. Hence, there exists a constant $N > 0$, such that when $c \geq N$, $b(\eta, c) > -1$ uniformly for any $\eta \in [0, \alpha]$ and $Q(\eta, c)$ is well defined. Note that by this definition, for $b(\eta, c) > -1$,

$$\gamma_1 \cos\eta + \gamma_2 \sin\eta = \cosh(Q(\eta, c)) a(c).$$

Moreover, it can be seen from the definition that $Q(\eta, c)$ is continuous. Given the notation above, we are now in position to introduce Theorem 4.

Theorem 4. (i) *When $p \geq \max(M, N)$ (where M is defined in Condition 2(ii)) such that $b(\eta, c) > -1$ holds and $Q(\eta, p)$ is well defined, the joint moment of $-J_1(\varepsilon_p)$ and $-J_2(\varepsilon_p)$ is given by the following double integral:*

$$\begin{aligned}
&\mathbb{E}^{(0,0)}[(-J_1(\varepsilon_p))(-J_2(\varepsilon_p))] \\
&\quad = \sqrt{\frac{2}{\pi}} \frac{\sigma_1 \sigma_2 \sin\alpha}{(a(p))^2} \biggl(\int_{\eta=0}^{\alpha} \int_{\nu=0}^{\infty} \frac{\Gamma(2 - \mathrm{i}\nu)\Gamma(2 + \mathrm{i}\nu)}{\sinh(\alpha\nu)} \\
&\qquad \times [\cosh(\beta_1(c)\nu) \sinh((\alpha - \eta)\nu) + \cosh(\beta_2(c)\nu) \sinh(\eta\nu)] \\
&\qquad \times \frac{\mathbb{P}_{\mathrm{i}\nu - 1/2}^{-3/2}(\cosh(Q(\eta, p)))}{(\sinh Q(\eta, p))^{3/2}} \,\mathrm{d}\eta \,\mathrm{d}\nu \biggr),
\end{aligned}$$

with $p_1 = p_2 = v = \frac{1}{2} p$ in (17).

In particular, when $\mu_1 = \mu_2 = 0, \sigma_1 = \sigma_2 = 1$, the expression reduces to a result in [23] (the second to last equation therein), i.e.

$$\mathbb{E}^{(0,0)}[(-J_1(\varepsilon_p))(-J_2(\varepsilon_p))] = \frac{\sin\alpha}{p} \int_0^{\infty} \frac{\cosh((\pi/2 - \alpha)\nu)}{\sinh(\nu\pi/2)} \tanh\frac{\alpha\nu}{2} \,\mathrm{d}\nu.$$

(ii) When $\min(p_1, p_2) \geq \max(M, N)$ (where M is defined in Condition 2(ii)) such that $b(\eta, c) > -1$ holds and $Q(\eta, p_1 + p_2)$ is well defined, the joint moment of $-J_1(\varepsilon_{p_1})$ and $-J_2(\varepsilon_{p_2})$ is given by the following double integral:

$$\begin{aligned}
&\mathbb{E}^{(0,0)}[(-J_1(\varepsilon_{p_1}))(-J_2(\varepsilon_{p_2}))] \\
&\quad = \sqrt{\frac{2}{\pi}} \frac{\sin\alpha \sigma_1 \sigma_2}{(a(p_1 + p_2))^2} \biggl(\int_{\eta=0}^{\alpha} \int_{\nu=0}^{\infty} \frac{\Gamma(2 - \mathrm{i}\nu)\Gamma(2 + \mathrm{i}\nu)}{\sinh(\alpha\nu)} \\
&\qquad \times [\cosh(\beta_1(c)\nu) \sinh((\alpha - \eta)\nu) + \cosh(\beta_2(c)\nu) \sinh(\eta\nu)] \\
&\qquad \times \frac{\mathbb{P}_{\mathrm{i}\nu - 1/2}^{-3/2}(\cosh(Q(\eta, p_1 + p_2)))}{(\sinh Q(\eta, p_1 + p_2))^{3/2}} \,\mathrm{d}\eta \,\mathrm{d}\nu \biggr),
\end{aligned}$$

with $v = 0$ in (17).

Proof. See [29]. □

Acknowledgements

The authors are grateful to L. C. G. Rogers, Ning Cai, Xinyun Chen, Nan Chen, and an anonymous referee for their helpful comments and discussions. We would like to thank Ning Cai for kindly providing MATLAB programs for the inversion of the Laplace transforms. The research of Steven Kou is supported in part by MOE2014-T2-1-006 grant from MOE in Singapore, and R-2015-S-005 grant from NSFC in China.

References

[1] Abate, J. and Whitt, W. (1995). Numerical inversion of Laplace transforms of probability distributions. *ORSA J. Comput.* **7,** 36–43.
[2] Abramowitz, M. and Stegun, I. A. (1964). *Handbook of Mathematical Functions with Formulas, Graphs, and Mathematical Tables*. U.S. Government Printing Office, Washington, DC.
[3] Ben-Avraham, D. and Fokas, A. S. (1999). The solution of the modified Helmholtz equation in a wedge and an application to diffusion-limited coalescence. *Phys. Lett. A* **263,** 355–359.
[4] Cai, N., Kou, S. G. and Liu, Z. (2014). A two-sided Laplace inversion algorithm with computable error bounds and its applications in financial engineering. *Adv. Appl. Prob.* **46,** 766–789.
[5] Cheng, H., Huang, J. and Leiterman, T. J. (2006). An adaptive fast solver for the modified Helmholtz equation in two dimensions. *J. Comput. Phys.* **211,** 616–637.
[6] Ching, W.-K., Gu, J.-W. and Zheng, H. (2014). On correlated defaults and incomplete information. Preprint. Available at https://arxiv.org/abs/1409.1393.
[7] Downton, F. (1970). Bivariate exponential distributions in reliability theory. *J. R. Statist. Soc. B* **32,** 408–417.
[8] Freund, J. E. (1961). A bivariate extension of the exponential distribution. *J. Amer. Statist. Assoc.* **56,** 971–977.
[9] Gautschi W. (2006). Computing the Kontorovich–Lebedev integral transforms and their inverses. *BIT* **46,** 21–40.
[10] Giesecke, K. (2004). Correlated default with incomplete information. *J. Banking Finance* **28,** 1521–1545.
[11] Gumbel, E. J. (1960). Bivariate exponential distributions. *J. Amer. Statist. Assoc.* **55,** 698–707.
[12] Haberman, R. (2004). *Applied Partial Differential Equations*, 4th edn. Prentice Hall, Upper Saddle River, NJ.
[13] Haworth, H., Reisinger, C. and Shaw, W. (2008). Modelling bonds and credit default swaps using a structural model with contagion. *Quant. Finance* **8,** 669–680.
[14] He, H., Keirstead, W. P. and Rebholz, J. (1998). Double lookbacks. *Math. Finance* **8,** 201–228.
[15] Huh, J. and Kolkiewicz, A. (2008). Computation of multivariate barrier crossing probability and its applications in credit risk models. *N. Amer. Acturial J.* **12,** 263–291.
[16] Iyengar, S. (1985). Hitting lines with two-dimensional Brownian motion. *SIAM J. Appl. Math.* **45,** 983–989.
[17] Li, L. and Linetsky, V. (2015). Discretely monitored first passage problems and barrier options: an eigenfunction expansion approach. *Finance Stoch.* **19,** 941–977.
[18] Li, X. (2006). On solving boundary value problems of modified Helmholtz equations by plane wave functions. *J. Comput. Appl. Math.* **195,** 66–82.
[19] Marshall, A. W. and Olkin, I. (1967). A multivariate exponential distribution. *J. Amer. Statist. Assoc.* **62,** 30–44.
[20] Metzler, A. (2010). On the first passage problem for correlated Brownian motion. *Statist. Prob. Lett.* **80,** 277–284.
[21] Oberhettinger, F. (1972). *Tables of Bessel Transforms*. Springer, New York.
[22] Polyanin, A. D. and Zaitsev, V. F. (1995). *Handbook of Exact Solutions for Ordinary Differential Equations*. CRC, Boca Raton, FL.
[23] Rogers, L. C. G. and Shepp, L. (2006). The correlation of the maxima of correlated Brownian motions. *J. Appl. Prob.* **43,** 880–883.
[24] Sacerdote, L., Tamborrino, M. and Zucca, C. (2015). First passage times of two-dimensional correlated diffusion processes: analytical and numerical methods. Preprint. Available at http://arxiv.org/abs/1212.5287.
[25] Shampine, L. F. (2008). Vectorized adaptive quadrature in Matlab. *J. Comput. Appl. Math.* **211,** 131–140.
[26] Spitzer, F. (1958). Some theorems concerning 2-dimensional Brownian motion. *Trans. Amer. Math. Soc.* **87,** 187–197.
[27] Watson, G. N. (1944). *A Treatise on the Theory of Bessel Funtions*. Cambridge University Press.
[28] Zhou, C. (2001). An analysis of default correlations and multiple defaults. *Rev. Financial Studies* **14,** 555–576.
[29] Kou, S. and Zhong, H. (2016). *First-passage times of two-dimensional Brownian motion: online supplement.* Available at http://rmi.nus.edu.sg/about-us/profile/stevenkou/stevenkou.html.